Scanning Electron Microscopy of the Human Myocardium

S. Siew
Michigan State University

Utah State University
MERRILL-CAZIER LIBRARY

SCANNING ELECTRON MICROSCOPY OF THE HUMAN MYOCARDIUM

S. Siew

Department of Pathology, Michigan State University
East Lansing, MI

Abstract

Owing to the impossibility of fixation, in the human being, by means of perfusion in vivo and the rare availability of fresh comparatively intact hearts resected at transplantation, the possibility was explored of using post-mortem material in instances where the autopsies were performed within 2 hours of demise of the patients. Four cases were examined: 2 normal adult hearts and 2 hearts of hypertensive patients in the stage of decompensation. The hearts were fixed by means of perfusion with 2.5% glutaraldehyde in phosphate buffer, pH 7.4. Contiguous blocks were taken for light microscopy (LM) and scanning electron microscopy (SEM) from the left ventricular free wall of all 4 cases and of the impulse conducting system of the heart in the 2 normal hearts. The SEM material was processed by the osmium-thiocarbohydrazide-osmium method (O-T-O). There was good correlation between the LM and SEM findings. The left ventricular blocks were sectioned in the transverse axis and SEM showed a step-wise transection of the myofibrils. Z and M bands, mitochondria and myofilaments were identified at ultrastructural magnifications. The difference in vascularity between normal and hypertensive myocardium and the presence of para-arterial fibrosis in the latter were demonstrated by SEM. The SEM study of the impulse conducting system of the heart included the sinoatrial (SA) and atrioventricular (AV) nodes and the penetrating portion of the atrioventricular (AV) bundle of His. Characteristic pacemaker or "P" cells were identified in the nodes.

KEY WORDS: Scanning electron microscopy, Human Myocardium, Impulse Conducting System.

Address for correspondence:
Shirley Siew
Michigan State University, East Fee Hall A622
East Lansing, MI 48824
Phone no.: 517 353-3755

Introduction

Modern invasive cardiovascular techniques, such as open heart surgery and endomyocardial biopsy are a source of fresh human cardiac tissue which is suitable for ultrastructural examination. An ever increasing amount of valuable transmission electron microscopic (TEM) information has been accrued by this means (4). However, only a comparatively small quantity of myocardium can be obtained and there has been only one SEM study of surgically resected human myocardium (19). Furthermore, neither of the above procedures is likely to be undertaken in normal subjects and to yield normal control material.

Post mortem degeneration has been a considerable deterrent to the investigation of human autopsy myocardium by TEM. The necessity of taking 1mm blocks compounds the difficulty of identification of the small aggregates of specialized tissue which constitute the impulse conducting system of the heart. Credit must be given to James and Sherf, (8, 9, 10, 11) in particular, for their TEM studies of the SA node (8, 10) AV node (9) and the AV bundle of His (11) in human cardiac specimens obtained within 3 (8, 9, 10) or 4 hours (11) after death. Thornell and associates have made extensive multidisciplinary investigations of the conducting system of many species and have examined human post mortem Purkinje fibers by means of TEM (23).

The present investigation was undertaken to explore the application of SEM to the human heart with special reference to the impulse conducting system. There have been several elegant SEM studies of non-human mammalian "working" myocardium: mouse (7, 12, 16), rat (1, 2, 17, 22), rabbit (22), dog (20, 21), sheep (18), fetal lamb (22), but these have not included the conducting system. The external surface of extruded Purkinje fibers from the false tendons of bovine hearts has been studied by SEM (3). The ever expanding knowledge of the pathophysiology of this system makes it even more essential to have a clear understanding of its morphology.

Materials and Methods

This investigation involved 4 cases on whom autopsies were performed within 2 hours of demise of the patients. There were two normal cardiovascular control subjects and two hypertensive cases. See Table 1.

Table 1

	Age	Sex	Heart-Weight	Cardiac Pathology	Cause of Death
1.	20	F	275 gm	Within normal limits	Carcinoma liver
2.	22	M	300 gm	Within normal limits	Automobile accident; fractured skull
3.	60	M	500 gm	Hypertrophy & dilatation left ventricle	Inter-current infection
4.	56	F	460 gm	Hypertrophy & dilatation left ventricle	Cerebral Hemorrhage

The thoracic cage and pericardial sac were opened in the conventional manner. The heart and aorta were mobilized. An incision was made into the ascending aorta and the heart was flushed with normal saline, this was followed by perfusion with 2.5% glutaraldehyde in phosphate buffer, pH 7.4, first retrograde from the aorta and then by cannulation of the coronary arteries. Following perfusion, the heart was removed out of the pericardial sac by division of the pulmonary veins and the great vessels. It was immersed for 24 hours in 2.5% glutaraldehyde in phosphate buffer, pH 7.4. Thereafter, the left ventricle was opened and blocks were taken of the free wall through the columnae carneae. Each block was bisected with a sharp blade. One half was submitted for routine histology and the other one for scanning electron microscopy. The impulse conducting system was studied by SEM only in the control normal hearts. In order to examine the sino-atrial (SA) node, a modification of Lev and Watne's method (13) was used: - 4 longitudinal blocks of about 2cm in length were taken of the full thickness of the heart from the sinoatrial junction, extending beyond the intercaval band to the right atrial appendage. The technique of Lev et al (14) was applied to the taking of blocks of the atrioventricular (AV) node and bundle. 4 longitudinal blocks are obtained by this method. These were also bisected and contiguous blocks were submitted for routine histology and SEM. The SEM material was processed by means of the O-T-O technique (15); dehydrated in ascending concentrations of alcohol up to 100%; critical point dried with CO_2 and examined at 20kV in an Etec Autoscan.

Results

Normal adult left ventricle
SEM of the normal adult left ventricle, at a

Figure 1. SEM Normal Adult Left Ventricle E-cobblestone appearance of intact endocardium, CE-cut edge of endocardium, TE-tangential section through subendocardial tissue, CT-connective tissue strands in myocardium of transected columnae carneae. Note the presence of pinpoint openings of transected vessels in the columnae carneae.
Figure 2. SEM Transverse Section of Myocardium Note the rich vascularity (V) of normal myocardium.
Figure 3. LM Normal Myocardium E-endocardium, V-vascular spaces in intimate apposition to the myofibers.
Figure 4. SEM Normal Myocardium M-close aggregation of myofibers to form bundles or fasciculi, V-blood vessels.
Figure 5. SEM Transverse Section of Normal Cardiac Myocyte (Myofiber) M-myofiber, S-sarcolemma, F-step-wise transection of columns of longitudinally oriented myofibrils, Z-Z bands.
Figure 6. SEM Myofibrils-Longitudinal and Transverse Planes Z-Z bands, M-M bands, Mi-Mitochondria (Interfibrillar). Note myofilaments give rise to striation on longitudinal plane of myofibrils.

low magnification, shows the uniform cobblestone appearance of the luminal surface of the intact endocardium (Fig. 1). The cut surface of the endocardium is seen as a thin membrane around the circumference of the transected columnae carneae. In an area, where the plane of section has been more tangential, several layers of fine fibrils can be seen between the endocardial cells and the myocardium. The columnae carneae have been cut in the transverse axis. Occasional strands of connective tissue stand out on the cut surface and pinpoint openings of transected blood vessels can be discerned. The normal myocardium has a rich blood supply, with capillaries coming into intimate apposition to the myofibers (Fig. 2). Direct correlation to the LM appearance is shown in Fig. 3.

SEM of the transected columnae carneae, at higher magnification, shows that there is a close aggregation of the cardiac myocytes to form bundles or fasciculi (Fig. 4). Each muscle bundle is invested by a fine connective tissue sheath. Blood vessels are present in the interfascicular spaces. There is a lack of uniformity of size and shape of the individual myocytes on transverse section. The classical cylindrical appearance can be appreciated in comparatively few instances. Many of the myofibers are more angular and they may have a flattened or strap-like configuration. Polygonal forms are present. The outer surface of the myofiber is constituted by the sarcolemma (Fig. 5). Within the myocyte, there are longitudinally oriented columns of myofibrils, which are transected in a step-wise manner, presumably, at the level of the intercalated discs. As in the case of the myofibers, there is irregularity in the shape and size of the myofibrils with an angular or flattened morphology (Figs. 5,6). Stacks of mitochondria are
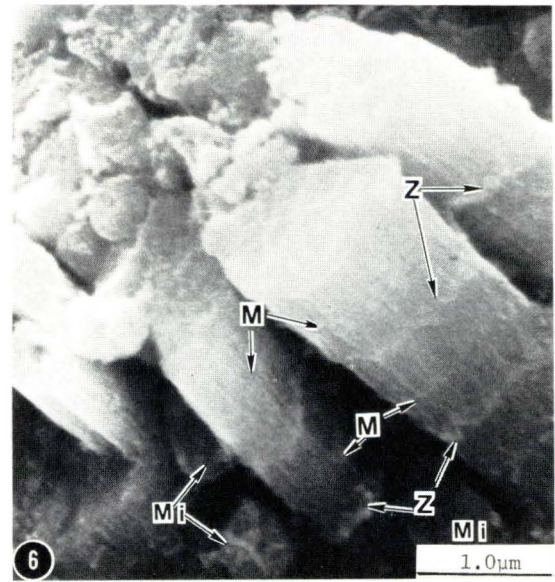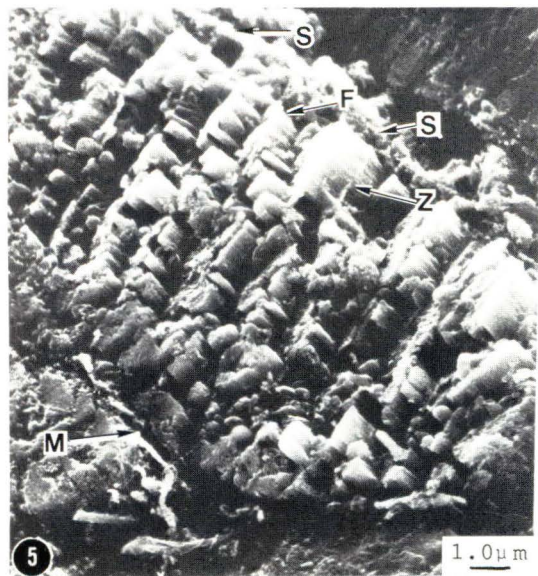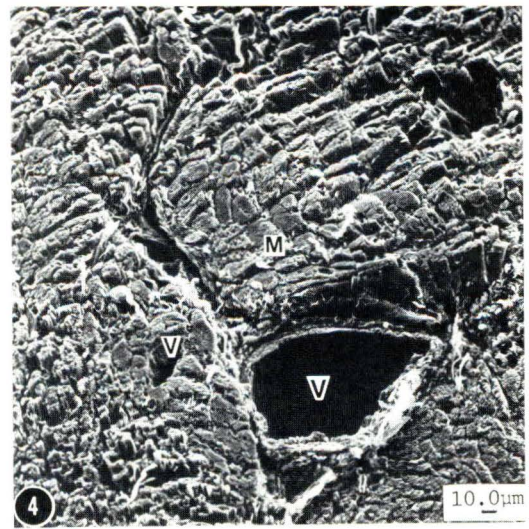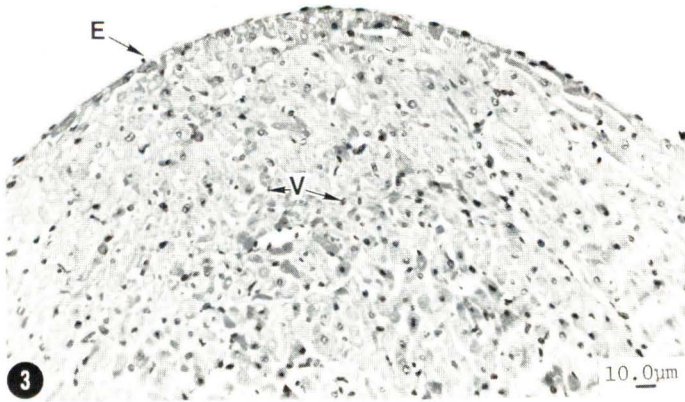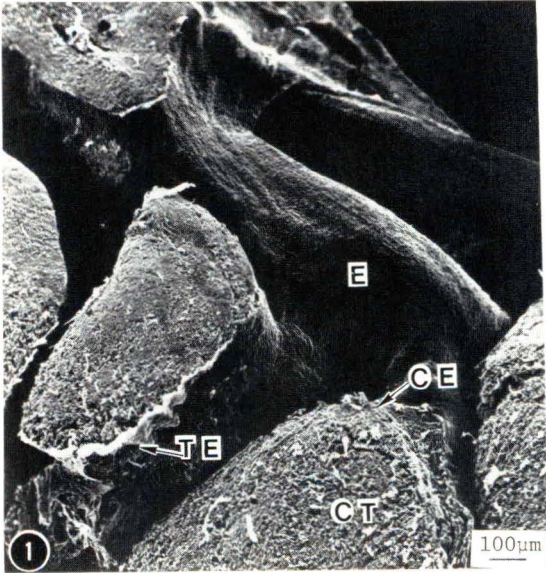
present between the myofibrils (interfibrillar mitochondria) (Fig. 6). There is also concentration of the mitochondria around the central nucleus (perinuclear mitochondria). The stepwise transection of the myofibrils allows their examination in both the longitudinal and transverse planes. In some instances, more than one sarcomere has been exposed on the longitudinal axis of the myofibrils. The Z bands give rise to prominent transverse ridges, located at regular intervals (Figs. 5,6). At high magnification M bands can be identified midway between the Z bands, as finer less continuous transverse bands, which have small nodules or knob-like excrescences (Fig. 6). In this aspect of the myofibril, the myofilaments give rise to a longitudinal striation of the surface. The cut edges of the myofilaments can be seen in the transverse plane of the myofibrils (Fig. 7). Rounded-ovoid interfibrillar mitochondria are present. A flattened structure has been observed extending, in the longitudinal axis, from the sarcolemma into the myofiber between the myofibrils. This could possibly be part of the longitudinal tubular system.

Hypertrophied and dilated left ventricle (Hypertrophy in the stage of decompensation).

SEM of the hypertrophied left ventricle shows an increase in the diameter of the columnae carneae (Fig. 8) in comparison to the normal, at the same magnification (Fig. 1). There is also thickening of the endocardium. Unlike the fine strands of connective tissue in the normal, there are occasional broad bands of fibrous tissue within the hypertrophied myocardium. The cut surface appears more dense with fewer pinpoint vascular openings but several large blood vessels are present. There is variation in the size and shape of the myofibers, with a notable increase of fibrous tissue between them (Fig. 9). Within the myocytes, there is a stepwise transection of the myofibrils. Nuclei are present in a central location and have been observed both in a transected and an intact state (Fig. 10). The SEM findings correspond to those of LM (Fig. 11) which shows endocardial thickening and para-arterial fibrosis of the myocardium.

Impulse Conducting System

Sino atrial (SA) node. The SA node can be identified at the lowest magnification by SEM, as an epicardial structure, which bridges the junction of the superior vena cava and the right atrium (Fig. 12). In this method of preparation, it has been sectioned longitudinally and it has a spindle or diamond shaped morphology, with a prominent central artery. At a higher magnification (Fig. 13), the SA node can be clearly distinguished from the fibroadipose tissue of the epicardium and from the right atrial myocardium. This bears out the low power LM appearance of the SA node (Fig. 14). The structure of the atrial myocardium is essentially similar to that of the left ventricle (Figs. 15,16). The myocytes contain large numbers of closely packed longitudinally oriented myofibrils (Fig. 16). The nodal cells are smaller. Their distribution is less regular with the formation of a plexiform network. There is also a greater quantity of

Figure 7. SEM Transected Myofilaments (Mf)
S-sarcolemma, LT-possibly part of longitudinal tubular system, Mi-mitochondria, Sa-sarcomeres. Shown in longitudinal axis.
Figure 8. SEM hypertrophied and Dilated Left Ventricle
E-thickened endocardium, CT-broad band of intramyocardial fibrous tissue.
Figure 9. SEM Hypertrophied and Dilated Left Ventricle
M-myofibers, F-step-wise transection of myofibrils, CT-connective tissue.
Figure 10. SEM Hypertrophied and Dilated Left Ventricle
M-myofiber, CT-connective tissue, N-prominent central nucleus.
Figure 11. LM Hypertrophied and Dilated Left Ventricle
E-thickened endocardium, M-myofibers, CT-connective tissue of para-arterial fibrosis.
Figure 12. SEM SA Node
Arrows point to the diamond shaped Node, CA-central artery, SVC-superior vena cava, RA-right atrium.

supporting tissue within the node. Some of the nuclei stand out clearly on the cut surface (Fig. 17). Higher magnification shows comparatively small polyhedral cells (Fig. 18). Because of the small size of these cells, the nuclei appear to be disproportionately large. The cytoplasm has a relatively empty appearance. Well formed myofibrils could not be identified in it. Scattered filaments and occasional mitochondria are present. It is considered that the morphological characteristics of these cells are in keeping with those of pacemaker or "P" cells. (8,10).

Atrioventricular (AV) node. The AV node is a subendocardial structure, which is located in the inferodistal part of the floor of the right atrium, adjacent to the base of the atrial septum, between the ostium of the coronary sinus and the septal cusp of the tricuspid valve. Its deep surface lies against the central fibrous body and its superficial surface is separated from the endocardium by several layers of right atrial myofibers (Figs. 19,20,21). There are blood vessels within the node and some adipose tissue. A few strands of fat cells are interposed between the nodal fibers and the central fibrous body. In this preparation, the AV node is seen in oblique section. It consists of a loose network of small fibers embedded in supporting tissue (Fig. 22). Higher magnification shows the presence of some myofibrils within the cells. There are also occasional small cells with disproportionately large nuclei and scanty myofilaments, showing the features of pacemaker or "P" cells (Fig. 23). (9).

The atrioventricular (AV) bundle of His. The penetrating portion of the AV bundle is a compact fine cord like structure which tunnels through the central fibrous body and is completely encased within the dense collagen of that body. It is rounded or roughly triangular on cross section. In its most distal position
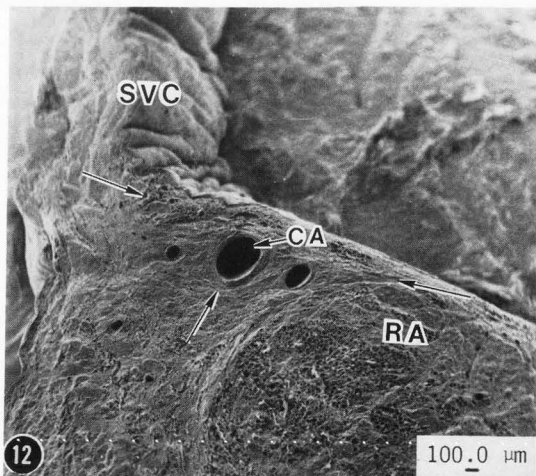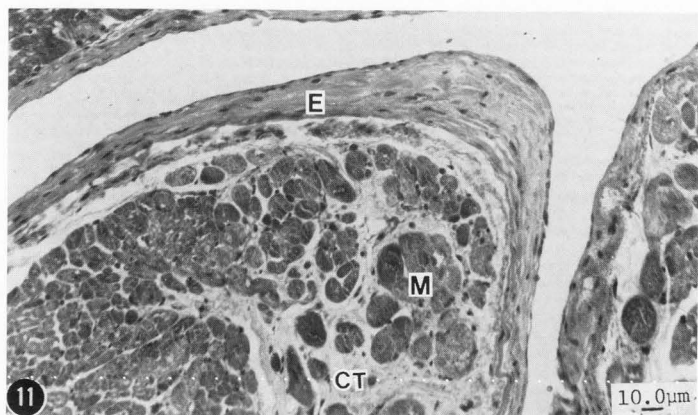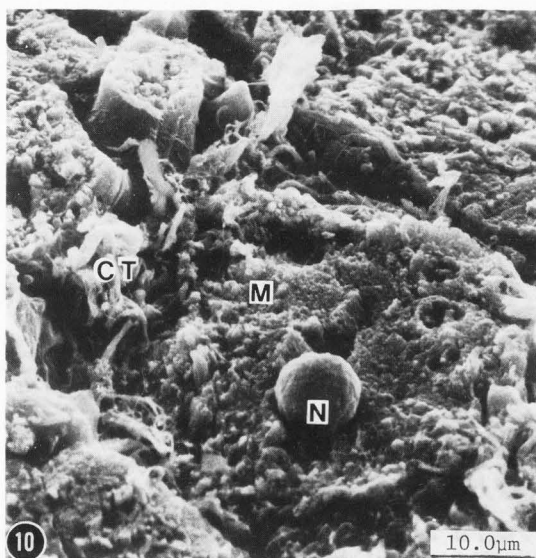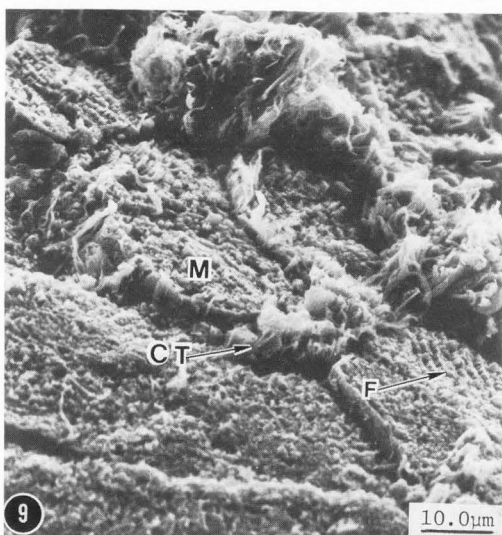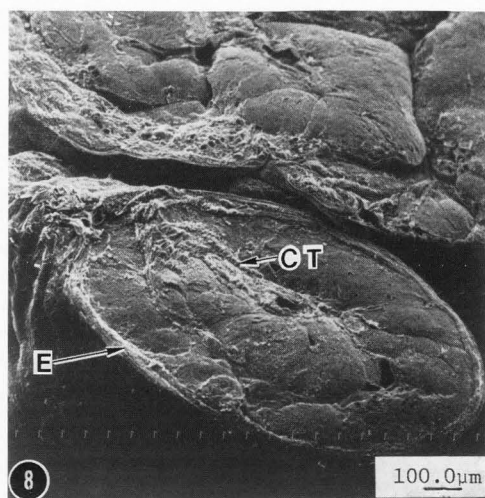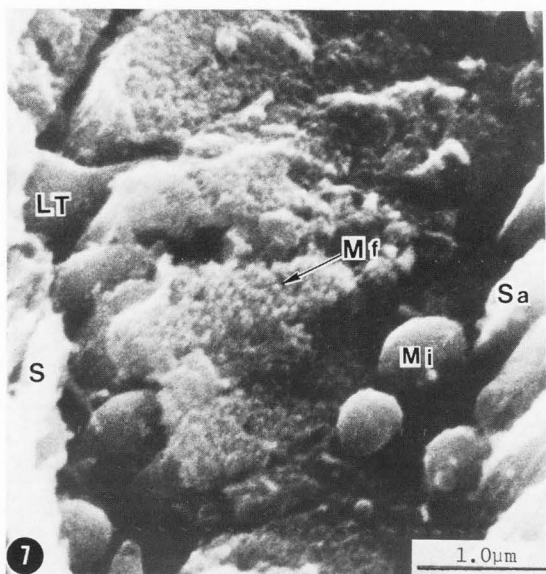
within the central fibrous body, the bundle lies immediately above the crest of the muscle of the interventricular septum (Figs. 24,25). In the plane in which it has been sectioned, it is seen as a well demarcated hemispherical structure, which tapers at its left superior pole, where it gives off the fascicles of the left bundle branch. Unlike the network of interweaving cells of the nodes, there is a more regular organization within the bundle, with parallel longitudinal orientation of the cells, partitioned by connective tissue septa (Figs. 26,27). The cells are elongated or ovoid in shape (Fig. 27). They contain more myofibrils than nodal cells but fewer than working myocytes. The typical stepwise myofibrillar transection is not prominent in the bundle. This could be due to the rarity of intercalated discs in the bundle fibers (11). Even at low magnification, there is a clear distinction between the AV bundle and the central fibrous body (Fig. 28). Higher magnifications demonstrate the dense collagenous structure of the central fibrous body (Fig. 29).

Discussion

In the preparation of non-human mammalian myocardium for SEM, cryofracture has been the method of choice (1,7,17,20,21,22) and the myofibers have been fractured in the longitudinal axis. By this means, many sarcomeres have been exposed and the transverse tubular or T-system has been studied in detail. Individual myofilaments have not been well demonstrated. It was postulated by Haggis (7) that they had probably become clumped together during freezing. SEM of deparaffinized sections of paraffin-embedded myocardium has been reported to give less satisfactory results (6,20).

In the present investigation, the tissues were processed by the "standard SEM procedure," in which the O-T-O method (15) was applied after fixation by perfusion. Blocks of normal and hypertrophied left ventricles were bisected in the transverse axis for correlative LM and SEM and good correlation was achieved. SEM shows a step-wise division of the myofibrils with limited exposure of the sarcomeres in the longitudinal axis. Regularly spaced Z bands and intervening M bands can be identified. Myofilaments are demonstrated more clearly on transverse section. Apart from the inference that the T-tubules are located at the Z bands, the transverse tubular system could not be resolved in this material. At high magnifications, a flattened structure was observed extending from the sarcolemma into the myofiber between the myofibrils (Fig. 7). This could possibly represent part of the longitudinal tubular system.

The differences between normal and hypertrophied myocardium in the state of decompensation or "degeneration" (4) are well demonstrated by SEM. The para-arterial fibrosis of the latter is quite distinct from the rich vascularity of normal myocardium (Fig. 2) and the concentric peri-arteriolar fibrosis of chronic rheumatic myocarditis (19). Owing to the variation in size and shape of the myofibers on transverse section, it would be difficult to obtain accurate

Figure 13. SEM SA Node.
Ep-epicardium, SA-SA node, V-blood vessel, RA-right atrium, A-adipocytes.
Figure 14. LM SA Node.
Ep-epicardium, SA-SA node, CA-central artery, RA-right atrium, A-adipocytes.
Figure 15. SEM Tail of Node and Right Atrium.
SA-SA node, Ep-epicardium, RA-right atrial myocardium.
Figure 16. SEM Right Atrial Myofibers in Transverse Section.
M-myofibers contain longitudinally oriented columns of myofibrils (F) which show step-wise transection, V-blood vessel.
Figure 17. SEM SA Node.
Ep-epicardium, SA-SA node, N-nuclei, RA-right atrium.
Figure 18. SEM SA Node - "P" Cell.
P-pacemaker or "P" cell. Polyhedral cell with disproportionately large nucleus-N. Relatively empty cytoplasm containing sparse filaments-Mf.

measurements of them. The range of normal myofiber width on TEM is given as 10 µm - 20 µm (4,5). There were fibers 30 µm in diameter in the hypertrophied ventricles. Left ventricular hypertrophy is a well recognized consequence of systemic hypertension. Its development in such patients carries a serious prognosis as it may be associated with significant disease of the coronary and cerebral circulations and followed by congestive heart failure. Much work remains to be done to elucidate the pathogenesis of myofiber hypertrophy and subsequent failure. SEM, particularly, using the stereologic technique, should prove helpful in differentiating between the addition of sarcomeres in parallel (pressure load) or in series (volume load).

Application of the methods of Lev and associates (13,14) has facilitated (in fact, insured) the LM identification of the impulse conducting system of the human heart. However, in depth studies necessitate serial sectioning and the examination of several thousand slides from each case. This becomes a time consuming undertaking, and, understandably, one that has been under utilized in view of the importance of demonstrating a morphological basis of arrhythmias. The significance of this cannot be overemphasized as fatal arrhythmias are responsible for 500,000 sudden unexpected cardiac deaths a year in the United States. The complexities of microscopic examination of the conducting system are considerably magnified at the TEM level.

SEM offers the facility of taking large blocks (2cm) of the impulse conducting system in accordance with the methods advocated for their histologic examination (13,14). By this means, there is good correlation between the LM and SEM findings. The distinction between conducting tissue and "working myocardium" is very clearly demonstrated by SEM (Fig. 13). Some of the features described by TEM (8,9,10,11) such as the ultrastructural characteristics of pacemaker or "P" cells are difficult to appreciate by LM but they are identified by SEM (Figs. 18,23).

While SEM has not given the resolution and detail of TEM, it has extended the observations

Figure 25

Figure 26

Figure 27

Figure 28

Figure 29
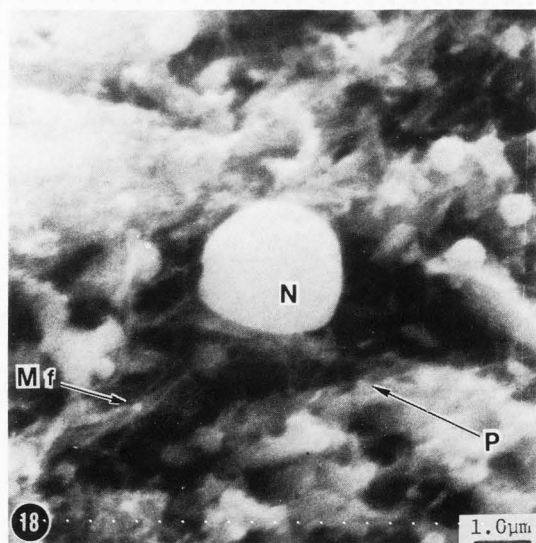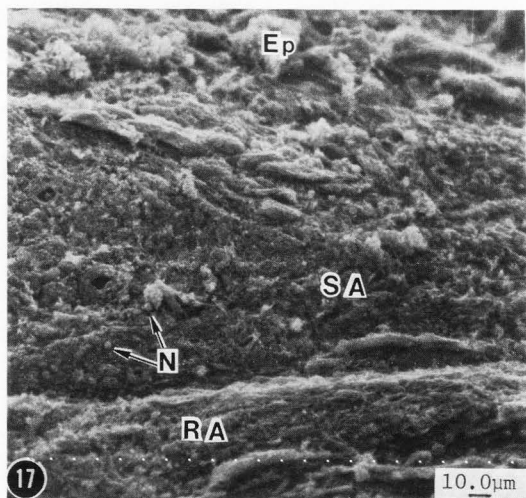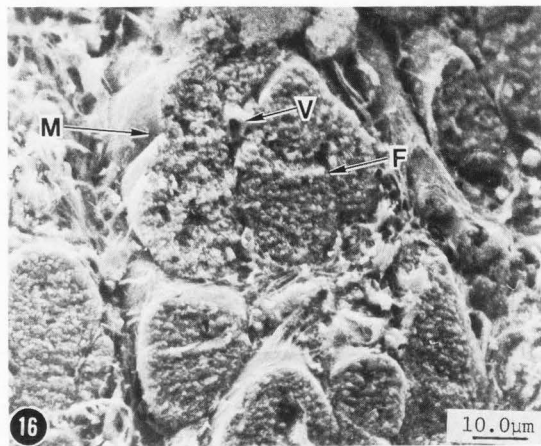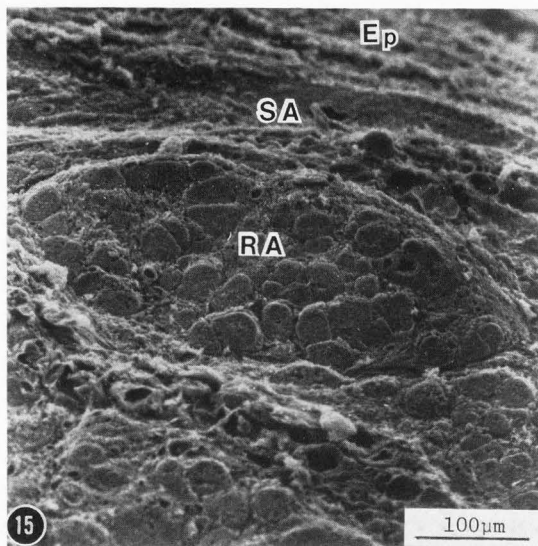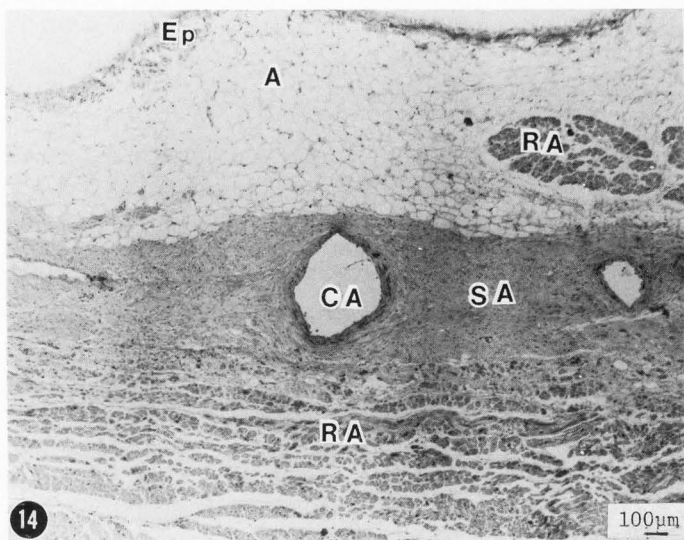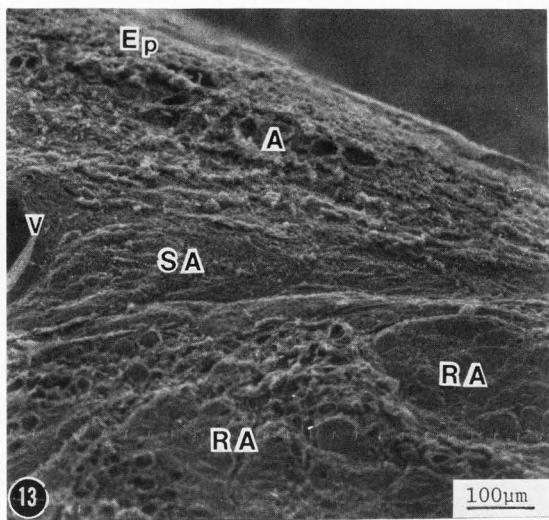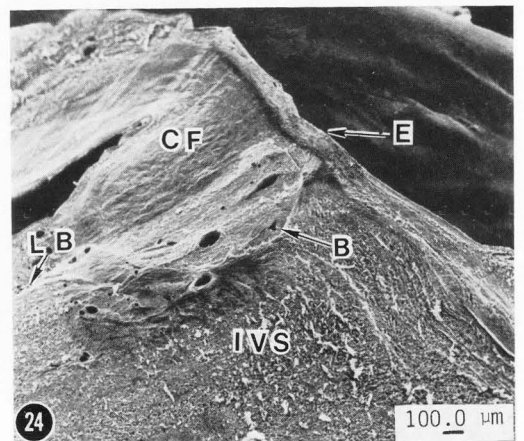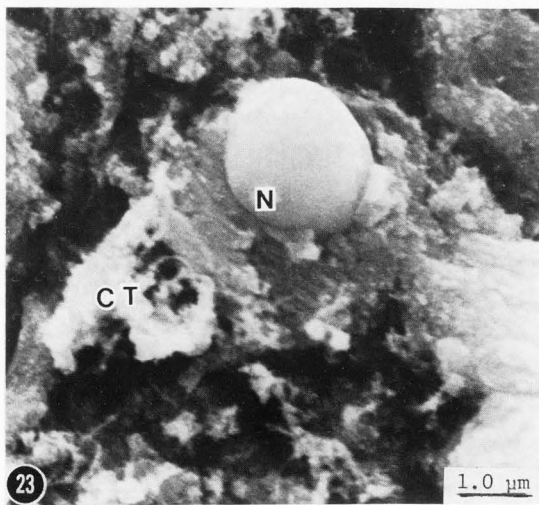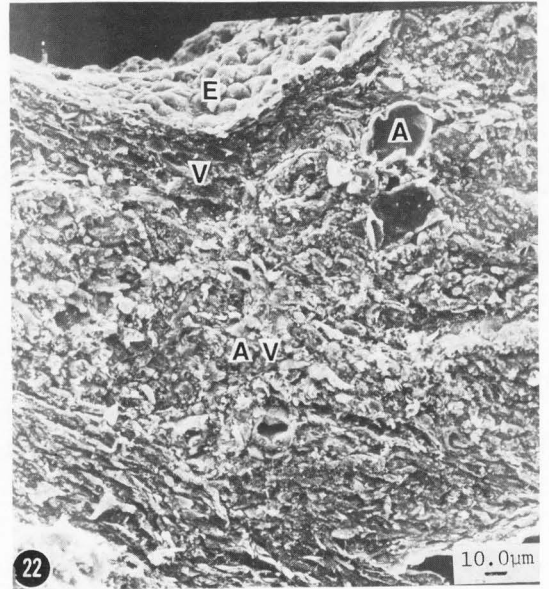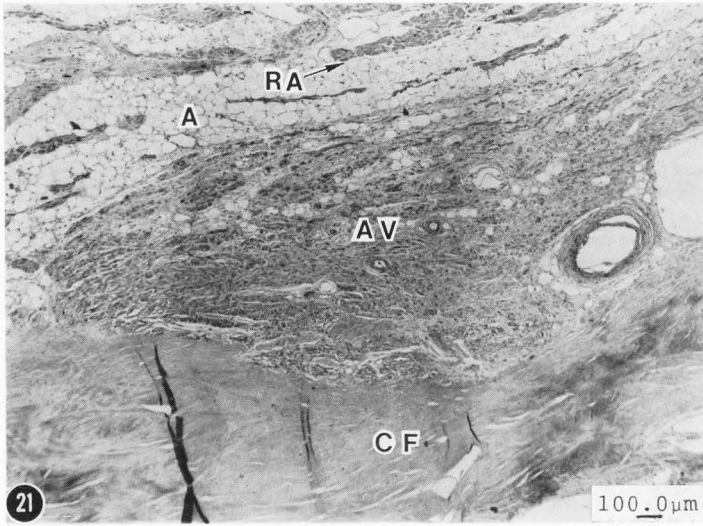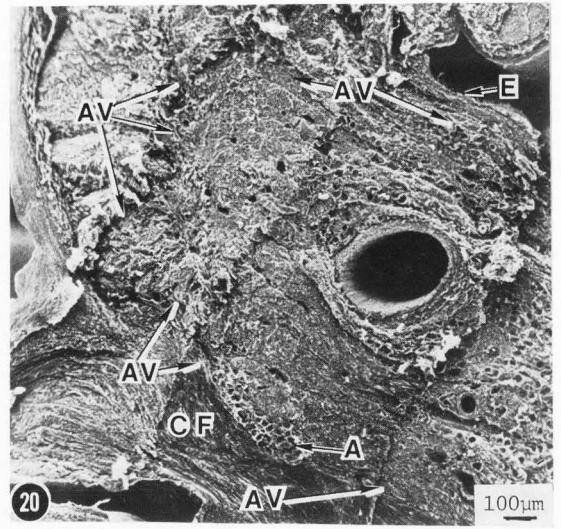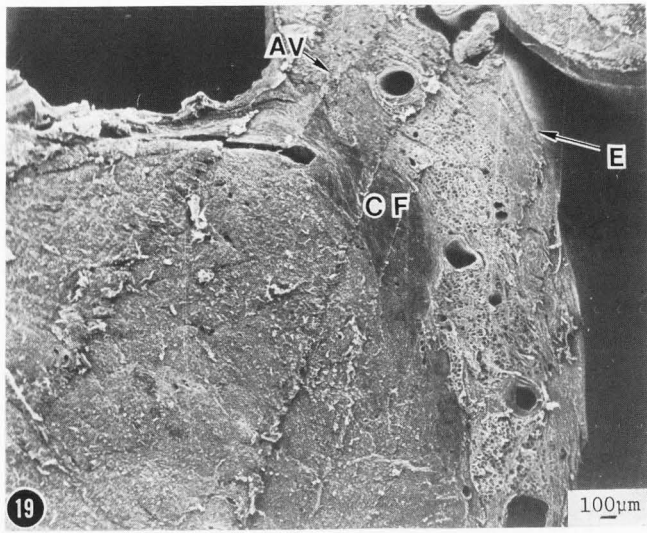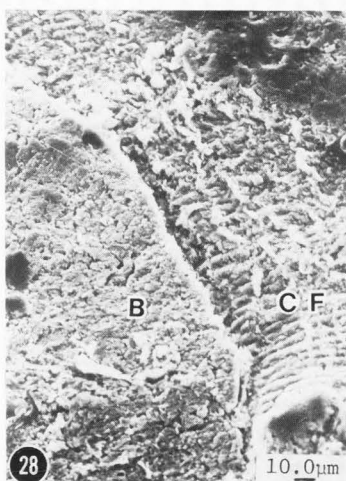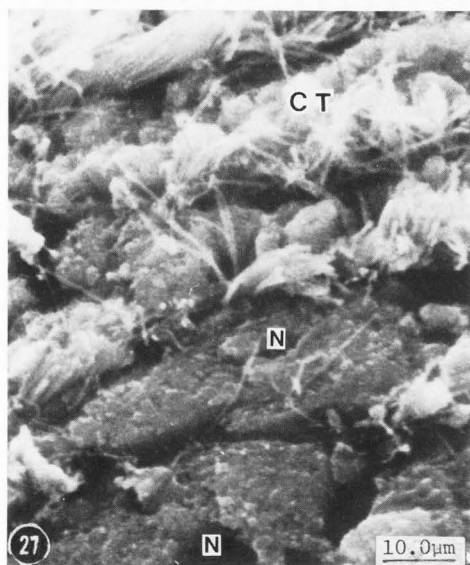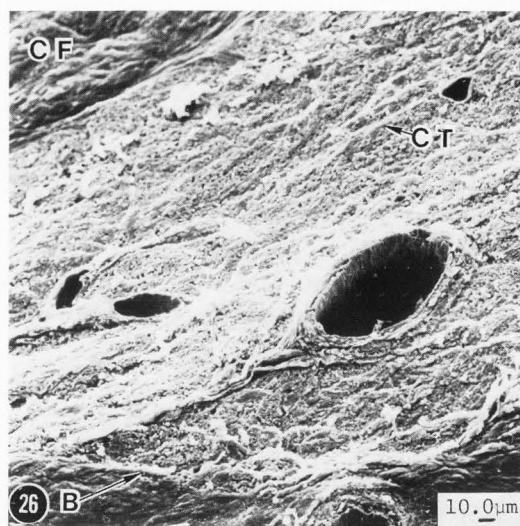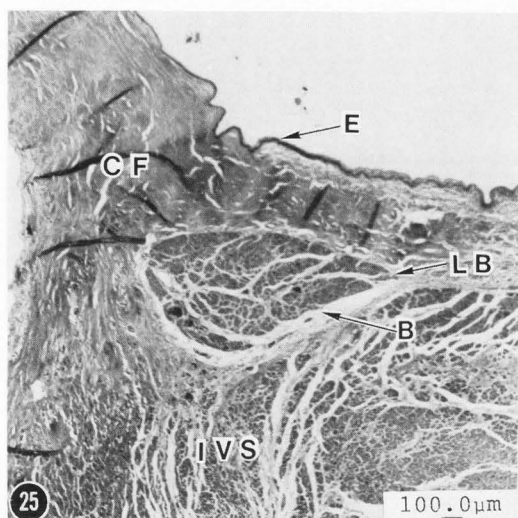
of LM to ultrastructural levels with the demonstration of myofibrils, Z and M bands, myofilaments and mitochondria, together with the additional advantage of the ability of SEM to render a three dimensional image.

References

1. Ashraf M, Sybers HD. (1974). Scanning electron microscopy of ischemic heart. Scanning Electron Microsc. 1974: 721-727.

2. Buss VH, Hanrath WK, Schoenmackers J. (1971). Uber rasterelektronemikroskopische Untersuchungen am Myokard der Ratte. Kreislaufforschg. 65, 58-69.

3. Eriksson A, Thornell L-E. (1979). Intermediate (skeletin) filaments in heart Purkinje fibers. J. Cell Biol. 80, 231-247.

Figures 19-21. AV node (SEM and LM). AV-AV node, CF-central fibrous body, E-endocardium right atrium, A-adipose tissue, RA-strands of right atrial myofibers.
Figure 22. SEM AV Node. AV-AV node showing a loose network of small fibers embedded in supporting tissue, V-blood vessel wall, E-endothelium of blood vessel, A-adipocytes.
Figure 23. SEM "P" Cell. Small, round-ovoid cell with disproportionately large nucleus-N. CT-connective tissue.
Figures 24 and 25. Penetrating portion of AV Bundle (SEM and LM). B-hemispherical section of AV bundle, LB-fascicles of left bundle branch, CF-central fibrous body, IVS-intraventricular septum, E-endocardium.
Figures 26-28. SEM AV Bundle. B-AV bundle, CF-central fibrous body, CT-connective tissue, N-large perinuclear zone. In Figure 26, note the regular orientation of cells partitioned by CT septa. In Figure 27, note ovoid or elongated cells separated by CT. In Figure 28, note the clear demarcation between the bundle and the CF.
Figure 29. SEM Central Fibrous Body. Dense collagen fibers.

4. Ferrans VJ, Butany JW. (1983). Ultrastructural pathology of the heart. in Diagnostic Electron Microscopy. Vol. 4. Trump BF, Jones RT. (eds) John Wiley & Sons, Inc. New York. 319-473.

5. Ferrans VJ, Thiedemann K-U. (1983). Ultrastructure of the normal heart in Cardiovascular Pathology. Vol I. Silver MD, (ed). Churchill Livingstone, New York. 31-86.

6. Geissinger HD. (1971). Correlated light optical and scanning electron microscopy of Gram smears of bacteria and paraffin sections of cardiac muscle. J. Microsc. 92, 2:109-117.

7. Haggis GH. (1970). Cryofracture of biological material. Scanning Electron Microsc. 1970: 97-104.

8. James TN, Sherf L, Fine G, Morales AR. (1966) Comparative ultrastructure of the sinus node in man and dog. Circulation, 34, 139-163.

9. James TN, Sherf L. (1968). Ultrastructure of the human atrioventricular node. Circulation, 37, 1049-1070.

10. James TN, Sherf L. (1968). Ultrastructure of myocardial cells. Am. J. Cardiol. 22, 389-416.

11. James TN, Sherf L. (1971). Fine structure of the His bundle. Circulation, 44, 9-28.

12. Leak LV. (1970). Fractured surfaces of myocardial cells. J. Ultrastruct. Res. 31, 76.

13. Lev M, Watne AV. (1954). Method for routine histopathologic study of human sinoatrial node. Arch. Pathol. 57, 168-177.

14. Lev M, Widran J, Erickson EE. (1951). A method for the histopathologic study of the atrioventricular node, bundle, and branches. Arch. Pathol. 52, 73-83.

15. Malick LE, Wilson RB. (1975). Evaluation of a modified technique for SEM examination of vertebrate specimens without evaporated metal layers. Scanning Electron Microsc. 1975: 260-266.

16. McAlear JH, Kreutziger GO, Pease RFW. (1967). Combining scanning and transmission electron microscopy in the study of heart muscle freeze etched replicas. J. Cell Biol. 35, 89A.

17. McCallister LP, Mumaw VR, Munger BL. (1974). Stereo Ultrastructure of Cardiac Membrane Systems in the Rat Heart. Scanning Electron Microsc. 1974: 713-720.

18. Myklebust R, Dalen H, Saetersdahl TS. (1975). A comparative study in the transmission electron microscope and scanning electron microscope of intracellular structures in sheep heart muscle cells. J. Microsc. 105, 57-65.

19. Siew S. (1978). Scanning electron microscopy of acute rheumatic valvulitis. Scanning Electron Microsc. 1978; II: 341-348, 234.

20. Sybers HD, Ashraf M. (1973). Preparation of cardiac muscle for SEM. Scanning Electron Microsc. 1973: 341-348.

21. Sybers HD, Ashraf M. (1974). Scanning electron microscopy of cardiac muscle. Lab. Invest. 30, 4, 441-450.

22. Sybers HD, Sheldon CA. (1975). SEM techniques for cardiac cells in fetal, adult and pathologic heart. Scanning Electron Microsc. 1975: 275-280.

23. Thornell L-E, Eriksson A. (1976). The ventricular conduction system - ultrastructure and function. Forensic Sci. 8, 1, 97-102.

Discussion with Reviewers

S. Glagov: Frozen-fracture preparations have been useful for examining the organization of the artery wall. Has the author tried this approach with the myocardium?
Author: We tried the freeze-fracture method in the preparation of skeletal muscle for SEM and found that the "standard SEM procedure" gave us better results, so we have not tried this approach with the myocardium.

S. Glagov: What aspects of myocardial disease, particularly those dealing with conducting problems, does the author believe are amenable to selective SEM study of the conducting system?
Author: The potential of SEM has been virtually unexplored in the investigation of cardiomyopathies. SEM should prove to be particularly helpful in the study of myofiber architecture in hypertrophic cardiomyopathy. There is practically an unlimited application of SEM in the study of conduction problems. The most important aspect would be the arrhythmia(s) responsible for sudden unexpected cardiac death.

M. Ashraf: There should be mitochondria around the nucleus in Fig. 10. Can the author comment on this? A crater like structure (at 2 o'clock) in the vicinity of "N" appears to be a fractured nucleus lying within a cell.
Author: The structure labeled "N" has the features of a nucleus because of its location in the center of the myofiber and its size - 8μm in diameter, which is too large for a mitochondrion. The myofiber ("M") has a longitudinal fracture, which has resulted in a deep cleft that extends beyond "N" almost to the sarcolemma. "N" is protruding out of this cleft above the cut surface of the myofiber. This appearance suggests that the force of transecting this block split the myofiber and led to extrusion of the nucleus but did not dislocate the perinuclear mitochondria which have remained deep to the transected surface of the myofiber. The smaller, crater like structure at 2 o'clock is in the peripheral zone of the myofiber and it is probably a vacuole.